Dynamic State Estimation Based Unit Protection

Boqi Xie[1], *Student Member, IEEE,* A. P. Sakis Meliopoulos[1], *Fellow, IEEE*
George Cokkinides[1], *Member, IEEE*, Jiahao Xie[1], *Student Member, IEEE*
Chiyang Zhong[1], *Student Member, IEEE,* Yu Liu[2], *Member, IEEE,* and Thibault Prevost[3], *Member, IEEE*
1. School of Electrical and Computer Engineering, Georgia Institute of Technology, Atlanta, Georgia 30332-0250, USA
2. School of Information Science and Technology, ShanghaiTech University, Shanghai, 201210, China, 3. RTE, France
Email: bxie34@gatech.edu

***Abstract*—The introduction of new data acquisition systems, i.e., merging units, provides more accurate data to protection schemes enabling faster and more reliable protection. This paper presents an object-oriented dynamic state estimation based protection (DSEBP) scheme on a protection unit using the measurements obtained from merging units. The DSEBP uses instantaneous measurements and adopts a detailed and object-oriented model that represents the protection zone, which may comprise two or more devices, and performs dynamic state estimation to determine whether an internal fault has occurred. The dynamic state estimation provides the best estimate of the protection zone states as well as the probability that the un-faulted protection zone model fits the measurements. When the probability drops below a certain threshold, a trip decision is issued with a user selected time delay. The DSEBP requires few settings (e.g., trip delay time, etc.) and is applicable to any combination of devices in the protection zone. This paper uses an example consisting of a transformer and a cable in a substation to substantiate the effectiveness of this method.**

***Index Terms*—dynamic state estimation based protection, unit protection, object-orientation, transformer and cable**

I. Introduction

Power system is continuously subject to faults and failures that may cause damages to power equipment and even threaten the safety of human beings. To prevent these damages, the power system is partitioned into a number of small portions called protection zones. Each protection zone is protected by a protection system that is responsible for any fault occurring in the protection zone while ignoring the faults outside the protection zone [1]. Most protection zones contain one device to be protected and the breakers/reclosers that are able to disconnect the device from the rest of the system. However, some protection zones consist of multiple devices, and the protection scheme is responsible for protecting all the devices in this protection zone, which is called unit protection. For example, in some cases a generator and the connected transformer (without breakers connecting in between) are considered as a single protection zone [2]. Another example is a transformer-and-cable unit in a substation [3]. As the connected cable is usually short, typically less than 1000 feet, there is no need to protect the transformer and the cable separately. Thus, the transformer and the associated cable are considered as a single protection zone. The reasons for such protection design are: 1) cost efficiency. Less breakers are required to be placed for a protection unit containing multiple devices. 2) If a fault occurs in either device, the other devices do not serve a purpose if they remain connected while the faulted device is disconnected. Hence, there is no point in protecting the two devices separately, and they should be disconnected as a whole unit under faults in any of the devices in the unit.

In recent years, a new protection scheme called dynamic state estimation based protection (DSEBP) is proposed and developed [4]. The main procedure of DSEBP is to 1) use instantaneous measurements obtained from merging units (MUs) and give the best estimate of the states in the protection zone, and 2) use estimated states to check the consistency between the measurements and the protection zone model. Inconsistencies occur if the physical circuit of the protection zone is changed, which indicates a fault in the zone. Since the external fault cannot change the physical circuit of the protection zone, the estimated states are continuously consistent with the zone model. Thus, the DSEBP is able to trip internal faults while ignoring external faults. Although many types of protection zone have been investigated and proved effective using DSEBP [5-7], only a single device is protected in all these protection zones. To accommodate all types of protection zone, the DSEBP should be able to work on unit protection in an object-oriented way. In addition, since DSEBP utilizes detailed models, the nonlinear parts such as transformer with saturable core should be considered.

This paper proposes an updated object-oriented DSEBP algorithm that processes unit protection with detailed nonlinear parts in a protection zone. The rest of the paper is organized as follows. Section II introduces an object-oriented approach to model all the devices in a protection zone. Section III describes a seamless construction of the protection zone measurement model and the dynamic state estimation based protection algorithm. Section IV employs an example provided by RTE, a utility in France, to demonstrate the protection scheme. Section V summarizes the effectiveness of the updated DSEBP scheme.

II. Object-Oriented Device Modeling Approach

Since the unit protection aims to protect multiple devices in a protection zone, to realize the full object-orientation in the protection algorithm, a general syntax is adopted to model all these devices in the zone, i.e., state algebraic quadratic companion form (SAQCF). This section introduces the procedure of such modeling approach.

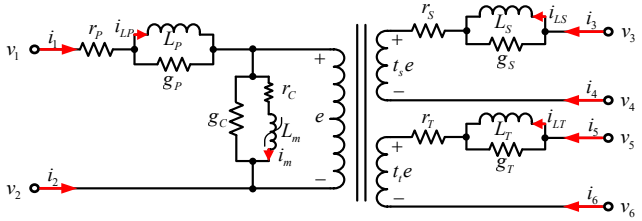

Figure 1: A Single-Phase Three-Winding Transformer with Saturable Core

A. Quadratized Device Model

The modeling approach starts from deriving equations reflecting the physical circuit of a device. For instance, as

978-1-7281-1981-6/19/$31.00 ©2019 IEEE

shown in Fig. 1, a single-phase three-winding transformer with saturable core is modelled in three equation sets, that is, terminal equation set, linear internal equation set, and nonlinear internal equation set. Because of page limitations, only the terminal equation set is provided as listed in (1).

$$\begin{cases} i_1 = i_{LP} + g_P L_P i'_{LP} + g_P M_{PS} i'_{LS} + g_P M_{PT} i'_{LT} \\ i_2 = -i_{LP} - g_P L_P i'_{LP} - g_P M_{PS} i'_{LS} - g_P M_{PT} i'_{LT} \\ i_3 = i_{LS} + g_S L_S i'_{LS} + g_S M_{PS} i'_{LP} + g_S M_{ST} i'_{LT} \\ i_4 = -i_{LS} - g_S L_S i'_{LS} - g_S M_{PS} i'_{LP} - g_S M_{ST} i'_{LT} \\ i_5 = i_{LT} + g_T L_T i'_{LT} + g_T M_{PT} i'_{LP} + g_T M_{ST} i'_{LS} \\ i_6 = -i_{LT} - g_T L_T i'_{LT} - g_T M_{PT} i'_{LP} - g_T M_{ST} i'_{LS} \end{cases} \quad (1)$$

where the prime symbol denotes the derivative with respect to time t; i_1, i_2, i_3, i_4, i_5, i_6 are terminal currents at time t; v_1, v_2, v_3, v_4, v_5, v_6, i_{LP}, i_{LS}, i_{LT}, λ, and i_m are states at time t (6 terminal voltages, 3 current through inductances, and the magnetic flux linkage and the magnetizing current inside the magnetic core of the transformer); L_P, L_S, and L_T are leakage inductances; L_m is the magnetizing inductance; M_{PS}, M_{PT}, and M_{ST} are mutual inductances; r_P, r_S, r_T and r_C are resistances; g_P, g_S, and g_T are stabilizers [8]. Note that the mutual inductances are not depicted in Fig. 1.

To fully describe the characteristics of the transformer, saturable iron core is also modeled, where the magnetizing current is computed by magnetizing inductance and magnetic flux with high order terms as listed in (2). To maintain the consistency among devices and achieve full object-orientation, we choose to keep the highest order of nonlinear terms less or equal to two (quadratization). For example, (2) is replaced by (3) when the order n is 13.

$$0 = i_m - \lambda/L_m - i_0 (\lambda/\lambda_0)^n \quad (2)$$

$$\begin{aligned} 0 &= i_m - \lambda/L_m - i_0\, y_4 \lambda/\lambda_0 & 0 &= y_3 - y_2^2 \\ 0 &= y_1 - (\lambda/\lambda_0)^2 & 0 &= y_4 - y_2 y_3 \\ 0 &= y_2 - y_1^2 \end{aligned} \quad (3)$$

The derived single-phase three-winding transformer model equations after quadratizaiton is called the quadratized device model (QDM), which is also applicable to other devices in the power system. The general syntax of QDM is listed in (4), where $\mathbf{i}(t)$ is the terminal current (through variable) vector, $\mathbf{x}$ is the state variable vector at time t, Y_{x1} and Y_{x2} are linear coefficient matrices, D_{x1} is the coefficient matrix of differential terms associated with states, F^i_{x2} denotes quadratic terms, and C_1, C_2 are constant vectors. Note that the equations with differential terms are arranged in the first equation set, while equations with quadratic terms are in the second equation set.

$$\begin{aligned} \left[\mathbf{i}^{\mathrm{T}}(t) \quad \mathbf{0}\right]^{\mathrm{T}} &= Y_{x1}\mathbf{x} + D_{x1}\mathbf{x}' + C_1 \\ \mathbf{0} &= Y_{x2}\mathbf{x} + \begin{Bmatrix} \vdots \\ \mathbf{x}^{\mathrm{T}} F^i_{x2} \mathbf{x} \\ \vdots \end{Bmatrix} + C_2 \end{aligned} \quad (4)$$

B. SAQCF Device Model

As the dynamic state estimation in this paper requires algebraic device model, the differential terms in the quadratized device model have to be eliminated. To obtain higher fidelity, the quadratic integration method [9] is applied to (4) with time step 2h by assuming the modeling time step of (4) is h. The final expression of the device model after the quadratic integration is the so-called state algebraic quadratic companion form (SAQCF) as shown in (5).

$$\begin{aligned} \left[\mathbf{i}^{\mathrm{T}}(t) \quad \mathbf{0} \quad \mathbf{i}^{\mathrm{T}}(t-h) \quad \mathbf{0}\right]^{\mathrm{T}} &= Y_x \mathbf{x} + \begin{Bmatrix} \vdots \\ \mathbf{x}^{\mathrm{T}} F^i_x \mathbf{x} \\ \vdots \end{Bmatrix} + B \\ B &= N_x \mathbf{x}(t-2h) + M\mathbf{i}(t-2h) + C \end{aligned} \quad (5)$$

where $\mathbf{x} = \left[\mathbf{x}^{\mathrm{T}}(t) \quad \mathbf{x}^{\mathrm{T}}(t-h)\right]^T$,

$$Y_x = \begin{bmatrix} \frac{2}{h}D_{x1} + Y_{x1} & -\frac{4}{h}D_{x1} \\ Y_{x2} & 0 \\ \frac{1}{4h}D_{x1} & \frac{1}{h}D_{x1} + Y_{x1} \\ 0 & Y_{x2} \end{bmatrix},\ F_x = \begin{bmatrix} 0 & 0 \\ F_{x2} & 0 \\ 0 & 0 \\ 0 & F_{x2} \end{bmatrix},\ N_x = \begin{bmatrix} -Y_{x1} + \frac{2}{h}D_{x1} \\ 0 \\ \frac{1}{2}Y_{x1} - \frac{5}{4h}D_{x1} \\ 0 \end{bmatrix},$$

$$M = \begin{bmatrix} I & 0 & -1/2I & 0 \end{bmatrix}^T,\ C = \begin{bmatrix} 0 & C_2^T & 3/2C_1^T & C_2^T \end{bmatrix}^T.$$

III. Measurement Model and Dynamic State Estimation

This section presents a seamless procedure of creating the protection zone measurement model based on the device SAQCF models and the measurements from the merging units in this protection zone as shown in Fig. 2. Then, the dynamic state estimation works directly on the protection zone measurement model and releases the trip decision without any other interference.

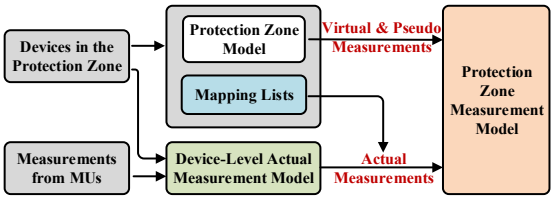

Figure 2: Overall Approach of Constructing the Zone Measurement Model

A. Device-Level Actual Measurement Model

Given the measurements from merging units and the device SAQCF models, the device-level actual measurement model can be directly constructed. For a voltage measurement, its measurement model is simply a linear combination of the states of the measured device plus a measurement error from this merging unit, i.e.,

$$z_v = A_v \mathbf{x} + \eta \quad (6)$$

where subscript v refers to the voltage measurement, z_v is the measurement value, A_v is the linear coefficient matrix, $\mathbf{x}$ is the device state vector, and η is the noise introduced by this merging unit. For a current measurement, its measurement model is obtained directly from the corresponding equation of the device SAQCF model, i.e.,

$$\begin{aligned} z_i &= Y_{ix}\mathbf{x} + \begin{Bmatrix} \vdots \\ \mathbf{x}^{\mathrm{T}} F^i_{ix} \mathbf{x} \\ \vdots \end{Bmatrix} + B_i + \eta \\ B_i &= N_{ix}\mathbf{x}(t-2h) + M_i i(t-2h) + C_i \end{aligned} \quad (7)$$

where subscript i refers to the current measurement, Y_{ix} is the linear coefficient matrix, F matrices are the nonlinear coefficient matrices, N_{ix} and M_i are linear coefficient matrices with respect to past-history terms, and C_i is the constant term.

B. Construction of the Protection Zone Measurement Model

Since DSEBP works on an object with SAQCF syntax [4], the protection unit should also be represented as an object in SAQCF syntax. To achieve this goal, we use the devices in the protection zone with SAQCF representation to construct the protection zone in the same syntax. With the protection zone

SAQCF model, we are able to create the protection zone level measurement model, which is processed by DSEBP. To construct the protection zone level measurement model, three tasks are performed: 1) Construct the zone-level SAQCF model and form the mapping lists (states, equations) from devices to the protection zone, 2) create the zone-level actual measurement model based on the formulated device-level actual measurement model and the mapping lists, and 3) create the zone-level virtual and pseudo measurement model using the zone-level SAQCF model.

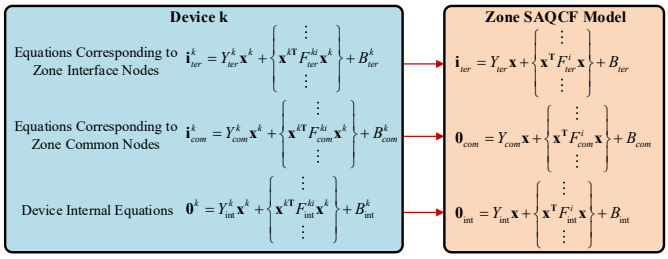

Figure 3: Protection Zone SAQCF Formulation

Given n device SAQCF models represented in (5) in the protection zone, the first task is to create the zone model in SAQCF syntax as shown in Fig. 3. In general, a device SAQCF model consists of three types of equations: a) equations corresponding to the zone interface nodes, b) equations corresponding to the zone common nodes, and c) device internal equations. To formulate zone SAQCF model, we keep types a and c equations and replace the states in terms of devices by the states in terms of the protection zone. For type b equations from different devices but corresponding to a same common node, we apply Kirchhoff's current law (KCL) at each node which provides one equation for each node and which eliminates the through variables. These equations are in terms of the states of the protection zone. During this task, we first create the mapping lists (states, equations) from devices to the protection zone based on the device connectivity. Then, the zone SAQCF model is automatically created by the device SAQCF models in this protection zone and the mapping lists. The output of this step is the zone SAQCF model as listed in Fig. 3. Note that in the zone SAQCF model, the equations with the current **i** on the left-hand side denote the currents flowing into the zone through the interface nodes, while all the other equations with zero value on the left-hand side are the device internal equations and the zero sum of equations at the common nodes derived from KCL.

The second task is to form the zone-level actual measurement model by using the formulated mapping lists that map the states and equations in the device-level actual measurement model to those in the zone-level actual measurement model. To achieve the observability and increase redundancy, the third task is then performed, which creates two other types of measurement model, i.e., virtual and pseudo measurement models. Virtual measurement models are provided by the protection zone internal equations reflecting the physical property (e.g., KCL, etc.) of the protection zone with high accuracy. These are directly obtained from the equations with zero value on the left-hand side in the zone-level SAQCF model with a relatively small measurement error compared to actual measurement models as shown in (8), where subscript *vm* refers to virtual measurement model. Pseudo measurement models are not directly measured but are quantities for which we know their approximate values. For example, the voltage at a neutral is around zero during normal operations. This voltage can be introduced as a pseudo measurement. Since we do not know the exact value of pseudo measurements, a relatively higher measurement error compared to the actual measurement model is introduced.

$$0 = Y_{vmx}\mathbf{x} + \begin{Bmatrix} \vdots \\ \mathbf{x}^{\mathrm{T}} F_{vmx}^{i} \mathbf{x} \\ \vdots \end{Bmatrix} + N_{vmx}\mathbf{x}(t-2h) + C_{vm} + \eta \qquad (8)$$

By following all these three tasks and combining zone-level actual, virtual, and pseudo measurement models, the final expression of the protection zone measurement model with a similar syntax as the zone SAQCF model is obtained:

$$\mathbf{z} = h(\mathbf{x}) + \boldsymbol{\eta} = Y_{zx}\mathbf{x} + \begin{Bmatrix} \vdots \\ \mathbf{x}^{\mathrm{T}} F_{zx}^{i} \mathbf{x} \\ \vdots \end{Bmatrix} + N_{zx}\mathbf{x}(t-2h) + M_{z}\mathbf{i}(t-2h) + C_{z} + \boldsymbol{\eta} \qquad (9)$$

C. *Dynamic State Estimation and Fault Detection*

The dynamic state estimation algorithm is applied on the formulated zone measurement model and provides the best estimate of the states at each time step by applying the weighted least square method:

$$Minimize \quad J = \left(h(\mathbf{x}) - \mathbf{z}\right)^{\mathrm{T}} W \left(h(\mathbf{x}) - \mathbf{z}\right) \qquad (10)$$

where W is a diagonal matrix with each diagonal element to be $1/\sigma_i^2$, and σ_i is the standard deviation (i.e., measurement error) of measurement i.

If the measurement model is nonlinear (the example case in Section IV), linearization technique is applied by assuming an initial guess $\mathbf{x}^{\nu}$, and the residual between the measurements and the linearized measurement model is:

$$\mathbf{r} = h\left(\mathbf{x}^{\nu}\right) + H\left(\mathbf{x}^{\nu}\right)\left(\mathbf{x} - \mathbf{x}^{\nu}\right) - \mathbf{z} = H\left(\mathbf{x}^{\nu}\right)\mathbf{x} - \mathbf{b} \qquad (11)$$

where $\mathbf{b} = -h\left(\mathbf{x}^{\nu}\right) + H\left(\mathbf{x}^{\nu}\right)\mathbf{x}^{\nu} + \mathbf{z}$, $H\left(\mathbf{x}^{\nu}\right)$ is the Jacobian matrix of $h(\mathbf{x})$ at $\mathbf{x}^{\nu}$, and it is denoted as H for simplicity in the following paragraphs.

Now the objective function is in a linear form:

$$Minimize \quad J = \left(H\mathbf{x} - \mathbf{b}\right)^{\mathrm{T}} W \left(H\mathbf{x} - \mathbf{b}\right) \qquad (12)$$

where $\mathbf{x}$ is obtained from the solution of the necessary condition (i.e., $dJ/d\mathbf{x}=0$), and the solution is achieved by the iterative equation in (13). As the measurement model consists of the measurements at time t and t-h, the dynamic state estimation is performed using two consecutive measurements from MUs. In addition, the past history terms $\mathbf{x}(t\text{-}2h)$ and $\mathbf{i}(t\text{-}2h)$ are updated by the estimated $\mathbf{x}(t)$ and $\mathbf{i}(t)$ after each dynamic state estimation.

$$\mathbf{x}^{\nu+1} = \mathbf{x}^{\nu} - \left(H^{T} W H\right)^{-1} H^{T} W \left(h\left(\mathbf{x}^{\nu}\right) - \mathbf{z}\right) \qquad (13)$$

After the solution is obtained, the chi-square test is performed. The chi-square test is a mathematical method to check the consistency between the measurements and the zone model. The procedure is expressed in (14):

$$\xi = \sum_{i} \left(\left(h_i(\mathbf{x}) - z_i\right)/\sigma_i \right)^2 \qquad P = 1 - \Pr(\xi, n) \qquad (14)$$

where ξ is the chi-square value, n is the difference between the number of measurements and states (degree of freedom), $\Pr(\xi,n)$ is the probability function, and P is the confidence level evaluating if the measurements fit the zone model. A high confidence level (e.g., 100%) indicates the measurements

match the zone model, concluding that no fault exists in the protection zone. A low confidence level (e.g., 0%) denotes an inconsistency between the measurements and the zone model, which implies the protection zone is not in good health, i.e., the occurrence of an internal fault. The trip decision is issued based on a user-defined delay time and reset time in (15).

$$trip = \begin{cases} 1, \text{ if } \int_{t-t_{reset}}^{t} P(\tau)d\tau > t_{delay} \\ 0, \text{ otherwise} \end{cases} \quad (15)$$

Once an internal fault is detected, a hypothesis test is performed to determine which component in the unit is faulted. The hypothesis test is defined as: fault is in device *i* of the unit". To test each hypothesis, the algorithm removes all the measurements that depend on the model of device *i*. These measurements include through measurements and internal measurements in device *i*. The dynamic state estimation is rerun to check if the remaining measurements are consistent with the model of the remaining devices in the unit. If the confidence level goes back to 100%, then we draw the conclusion that the fault occurs in the removed component.

IV. Illustrative Results

This section uses an illustrative example to demonstrate the effectiveness of the proposed unit protection algorithm. The example case is a selected protection zone (shown in Fig. 4) located in a 225kV/90kV substation of RTE, France. Two events are simulated: Event 1 is an internal fault occurring at bus TRNS1~90 and event 2 is an external fault occurring outside the protection zone, but still in the substation (not shown in the figure). The proposed algorithm is expected to detect the internal fault and ignore the external fault. For each event, we generate a one-second COMTRADE file to store the measurements from MUs. The merging unit collects 80 samples per cycle. Since the base frequency is 50 Hz for this system, the total number of samples per second is 4000. Note that these sampled values are directly used in DSEBP. Because of page limits, only part of the simulation and protection results are shown in this paper.

A. Example Case Description

The protection zone consists of one three-phase three-winding transformer with saturable core, one underground cable, and bus TRNS1~90 connecting between them. Four MUs are installed to collect the voltage and current measurements of this protection zone. The parameters of the protection zone and the measurement channels of the four MUs are described in Table 1 and 2.

In this example, we have 15 voltage and 15 current measurements from MUs. In addition, DSEBP automatically creates the virtual and pseudo measurements: 1) 61 virtual measurements (57 being internal equations in the transformer and the cable, and 4 obeying KCL on phase A, B, C, N at TRANS1~90), and 2) 3 pseudo measurements (neutral voltage being close to zero at TRNS1~225, TRNS1~90 and CABLE1~90). In summary, we have 94 measurements. The observability of the protection zone is checked offline. Specifically, as the protection zone consists of 74 states and the rank of the protection zone measurement model is 74, the protection zone is observable. The redundancy is 94/74=127%.

Table 1: Parameters of the Protection Zone

Three-Phase Three-Winding Transformer			
Winding Specifications			
	Primary	Secondary	Tertiary
Rated Voltage (L-L)	225 kV	90 kV	10.5 kV
Connection Type	WYE	WYE	DELTA
Short Circuit Test Data (p.u.)			
	R	X	Base (MVA)
P-S	0.01307	0.1226	100.0
P-T	3.149074	22.6126	100.0
S-T	3.158	22.49	100.0
Core Parameters			
Nominal Core Loss	Nominal Magnetizing Current	Exponent of Nonlinear Magnetizing Current	
0.001 p.u.	0.001 p.u	13.0	
90 kV Cable			
Rated Voltage	Length	Ground Resistance	CSA per phase	CSA of the shield	Type
90.0 kV	76.2 m	50.0 Ω	20 cm^2	3.21 cm^2	Single-Core

Note: CSA stands for Cross Sectional Area.

Table 2: Measurement Channels of the MUs in the Protection Zone

MU Name	Voltage Channels	Current Channels	# of Channels of this MU
MU1	AN, BN, CN at TRNS1~225	A, B, C at TRNS1~225 (into the XFMR)	9
		A, B, C at TRNS1~T (into the XFMR)	
MU2	AN, BN, CN at TRNS1~90	A, B, C at TRNS1~90 (into the XFMR)	9
	AN, BN, CN at TRNS1~T		
MU3	AN, BN, CN at CABLE1~90	A, B, C at CABLE1~90 (into the cable)	6
MU4	AN, BN, CN at TRNS1~90	A, B, C at TRNS1~90 (into the cable)	6

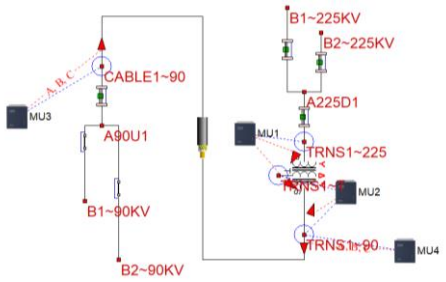

Figure 4: A Selected Protection Zone Provided by RTE, France

B. Event 1 – Internal Fault Case

Event 1 involves a phase A to neutral fault at TRNS1~90 bus within the protection zone. The fault is initiated at 0.5 seconds and cleared at 0.6 seconds in the simulation. The DSEBP is able to detect this internal fault and clear it by opening the breakers connected to this zone. Fig. 5 shows the measurements from MU2, and Fig. 6 shows selected measurements/estimated measurements from MU2, residuals between them, confidence level, and the trip decision in Event 1. We can observe that the confidence level drops down to zero immediately once the fault is initiated, i.e., the fault is detected immediately after the fault occurs. With the user defined trip reset time (300 ms) and delay time (10 ms), the DSEBP issues the trip decision in 10 ms and opens the breakers.

Once the internal fault is detected, hypothesis testing is performed to determine the faulted component. For this unit, three hypothesis tests are performed: 1) the fault occurs at bus TRNS1~90, 2) the fault occurs in the transformer, 3) the fault occurs in the cable. The first hypothesis test is performed by removing 4 virtual measurements at TRNS1~90 (KCL equations on phase A, B, C, N at TRNS1~90) and reruns the dynamic state estimation. The confidence level goes back to 100%. Thus, the internal fault of this unit is identified as a bus fault at TRNS1~90.

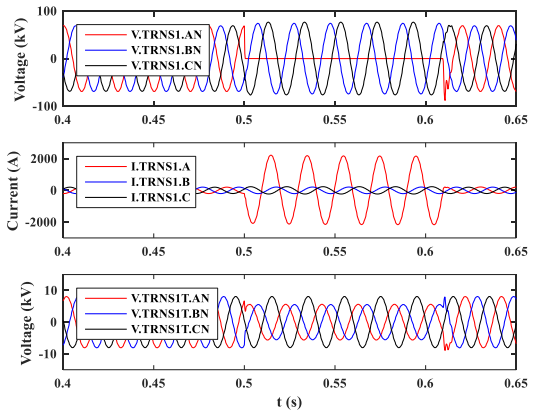

Figure 5: Measurements Obtained from MU2 in Event 1

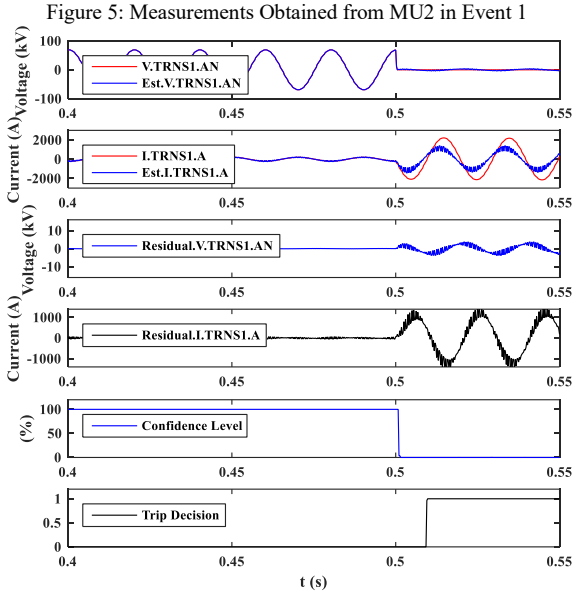

Figure 6: Residuals Between Selected Actual and Estimated Measurements from MU2, Confidence Level, and Trip Decision in Event 1

C. *Event 2 – External Fault Case*

Event 2 involves a phase A to neutral fault outside the protection zone but in the substation with the fault initiated at 0.5 seconds and cleared at 0.6 seconds. The DSEBP ignores this external fault. Fig. 7 shows the measurements from MU2, and Fig. 8 shows selected measurements and estimated measurements, residuals between them, confidence level, and the trip decision of the breakers in Event 2. As demonstrated in Fig. 8, the confidence level keeps 100% through the whole event. Therefore, no trip decision is released, and this external fault is successfully ignored.

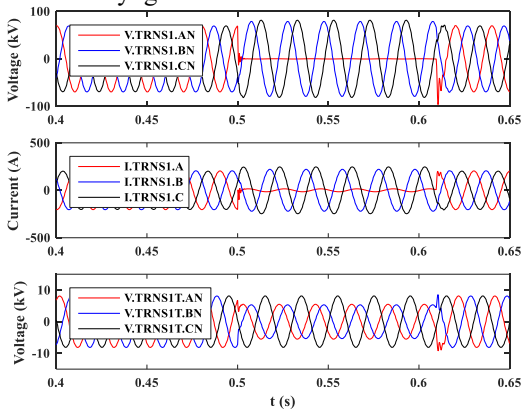

Figure 7: Measurements Obtained from MU2 in Event 2

V. Conclusions

This paper presents the dynamic state estimation based protection applicable to unit protection. The algorithm has the following features: 1) taking advantage of high sampling rate of the MU enables fast detection of faults, 2) introduction of virtual and pseudo measurements enhances the observability and further improves the accuracy of the estimated states in the protection zone, and 3) the object-oriented modelling approach enables the dynamic state estimation to process any combination of devices in the protection zone.

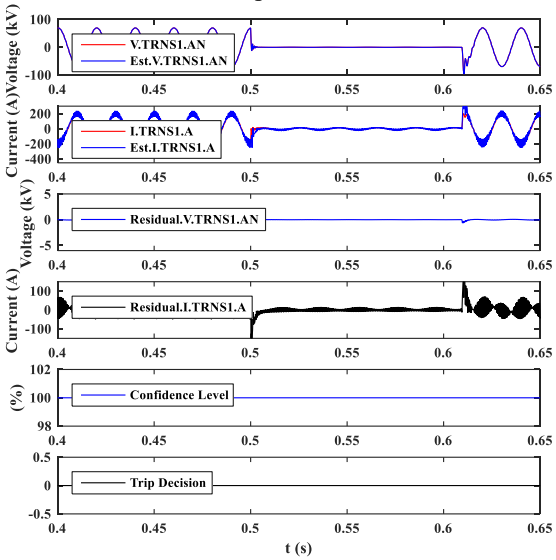

Figure 8: Residuals Between Selected Actual and Estimated Measurements from MU2, Confidence Level, and Trip Decision in Event 2

Acknowledgment

This work is supported by the Power Systems Engineering Research Center and RTE. Their support is greatly appreciated.

References

[1] P. M. Anderson, *Power System Protection*. New York: IEEE Press, 1999.

[2] J. H. Sykes, "The electrical protection of generators and transformers," in Students' Quarterly Journal, vol. 39, no. 153, pp. 3-7, September 1968.

[3] J. Cardenas, M. Kumar and J. Romero, "Problems and solutions of line differential application in cable + transformer protection," 10th IET International Conference on Developments in Power System Protection (DPSP 2010). Managing the Change, Manchester, 2010, pp. 1-5.

[4] A. P. S. Meliopoulos et al., "Dynamic State Estimation-Based Protection: Status and Promise," in IEEE Transactions on Power Delivery, vol. 32, no. 1, pp. 320-330, Feb. 2017.

[5] Y. Liu, A. P. S. Meliopoulos, R. Fan, L. Sun and Z. Tan, "Dynamic State Estimation Based Protection on Series Compensated Transmission Lines," in IEEE Transactions on Power Delivery, vol. 32, no. 5, pp. 2199-2209, Oct. 2017.

[6] L. Sun, R. Fan, A. P. S. Meliopoulos, Y. Liu and Z. Tan, "Capacitor bank protection via constraint WLS dynamic state estimation method (CWLS-DSE)," 2016 North American Power Symposium (NAPS), Denver, CO, 2016, pp. 1-6.

[7] J. Xie, A. P. S. Meliopoulos and B. Xie, "Transmission Line Fault Classification Based on Dynamic State Estimation and Support Vector Machine," 2018 North American Power Symposium (NAPS), Fargo, ND, USA, 2018, pp. 1-5.

[8] W. Gao, E. Solodovnik, R. Dougal, G. Cokkinides and A. P. S. Meliopoulos, "Elimination of numerical oscillations in power system dynamic simulation," Applied Power Electronics Conference and Exposition, 2003. APEC '03. Eighteenth Annual IEEE, Miami Beach, FL, USA, 2003, pp. 790-794 vol.2.

[9] G. K. Stefopoulos, G. J. Cokkinides and A. P. Meliopoulos, "Quadratic integration method for transient simulation and harmonic analysis," 2008 13th International Conference on Harmonics and Quality of Power, Wollongong, NSW, 2008, pp. 1-6.